

Measurement of Muon Neutrino Quasielastic Scattering on Carbon

A. A. Aguilar-Arevalo,⁵ A. O. Bazarko,¹² S. J. Brice,⁷ B. C. Brown,⁷ L. Bugel,⁵ J. Cao,¹¹ L. Coney,⁵ J. M. Conrad,⁵ D. C. Cox,⁸ A. Curioni,¹⁶ Z. Djurcic,⁵ D. A. Finley,⁷ B. T. Fleming,¹⁶ R. Ford,⁷ F. G. Garcia,⁷ G. T. Garvey,⁹ C. Green,^{7,9} J. A. Green,^{8,9} T. L. Hart,⁴ E. Hawker,¹⁵ R. Imlay,¹⁰ R. A. Johnson,³ P. Kasper,⁷ T. Katori,⁸ T. Kobilarcik,⁷ I. Kourbanis,⁷ S. Koutsoliotas,² E. M. Laird,¹² J. M. Link,¹⁴ Y. Liu,¹¹ Y. Liu,¹ W. C. Louis,⁹ K. B. M. Mahn,⁵ W. Marsh,⁷ P. S. Martin,⁷ G. McGregor,⁹ W. Metcalf,¹⁰ P. D. Meyers,¹² F. Mills,⁷ G. B. Mills,⁹ J. Monroe,⁵ C. D. Moore,⁷ R. H. Nelson,⁴ P. Nienaber,¹³ S. Ouedraogo,¹⁰ R. B. Patterson,¹² D. Perevalov,¹ C. C. Polly,⁸ E. Prebys,⁷ J. L. Raaf,³ H. Ray,⁹ B. P. Roe,¹¹ A. D. Russell,⁷ V. Sandberg,⁹ R. Schirato,⁹ D. Schmitz,⁵ M. H. Shaevitz,⁵ F. C. Shoemaker,¹² D. Smith,⁶ M. Sorel,⁵ P. Spentzouris,⁷ I. Stancu,¹ R. J. Stefanski,⁷ M. Sung,¹⁰ H. A. Tanaka,¹² R. Tayloe,⁸ M. Tzanov,⁴ R. Van de Water,⁹ M. O. Wascko,¹⁰ D. H. White,⁹ M. J. Wilking,⁴ H. J. Yang,¹¹ G. P. Zeller,⁵ and E. D. Zimmerman⁴

(MiniBooNE Collaboration)

¹University of Alabama, Tuscaloosa, Alabama 35487, USA

²Bucknell University, Lewisburg, Pennsylvania 17837, USA

³University of Cincinnati, Cincinnati, Ohio 45221, USA

⁴University of Colorado, Boulder, Colorado 80309, USA

⁵Columbia University, New York, New York 10027, USA

⁶Embry-Riddle Aeronautical University, Prescott, Arizona 86301, USA

⁷Fermi National Accelerator Laboratory, Batavia, Illinois 60510, USA

⁸Indiana University, Bloomington, Indiana 47405, USA

⁹Los Alamos National Laboratory, Los Alamos, New Mexico 87545, USA

¹⁰Louisiana State University, Baton Rouge, Louisiana 70803, USA

¹¹University of Michigan, Ann Arbor, Michigan 48109, USA

¹²Princeton University, Princeton, New Jersey 08544, USA

¹³Saint Mary's University of Minnesota, Winona, Minnesota 55987, USA

¹⁴Virginia Polytechnic Institute & State University, Blacksburg, Virginia 24061, USA

¹⁵Western Illinois University, Macomb, Illinois 61455, USA

¹⁶Yale University, New Haven, Connecticut 06520, USA

(Received 8 June 2007; published 23 January 2008)

The observation of neutrino oscillations is clear evidence for physics beyond the standard model. To make precise measurements of this phenomenon, neutrino oscillation experiments, including MiniBooNE, require an accurate description of neutrino charged current quasielastic (CCQE) cross sections to predict signal samples. Using a high-statistics sample of ν_μ CCQE events, MiniBooNE finds that a simple Fermi gas model, with appropriate adjustments, accurately characterizes the CCQE events observed in a carbon-based detector. The extracted parameters include an effective axial mass, $M_A^{\text{eff}} = 1.23 \pm 0.20$ GeV, that describes the four-momentum dependence of the axial-vector form factor of the nucleon, and a Pauli-suppression parameter, $\kappa = 1.019 \pm 0.011$. Such a modified Fermi gas model may also be used by future accelerator-based experiments measuring neutrino oscillations on nuclear targets.

DOI: [10.1103/PhysRevLett.100.032301](https://doi.org/10.1103/PhysRevLett.100.032301)

PACS numbers: 25.30.Pt, 13.15.+g, 14.60.Lm, 14.60.Pq

The recent observation of neutrino oscillations is strong evidence for massive neutrinos and, therefore, for physics beyond the standard model. Accelerator-based experiments searching for neutrino oscillations, such as MiniBooNE [1] and K2K [2], use charged current quasielastic (CCQE) interactions to search for the appearance of electron neutrinos ($\nu_e n \rightarrow e^- p$) in beams of muon neutrinos. The muon neutrino CCQE interaction ($\nu_\mu n \rightarrow \mu^- p$) thus provides a calibration for the neutrino beam and for the interaction cross section. In addition, such events dominate at energies between 200–2000 MeV where the oscillation searches are conducted. To ensure high event yields,

these experiments use nuclear media (carbon or water) as the neutrino target; therefore, it is crucial to employ an accurate model of the CCQE interaction on nuclei. In this Letter, we describe the model improvements developed for the recent oscillation search from the MiniBooNE experiment [1]. The modified model describes this reaction remarkably well and should be relevant for future accelerator-based neutrino oscillation searches.

To model the scattering from nucleons confined in nuclei, most neutrino oscillation experiments employ an event generator based on the relativistic Fermi gas (RFG) model [3]. Such models assume a flat nucleon momentum

distribution up to some Fermi momentum (p_F), assign a single value for the nucleon binding energy (E_B) to account for the initial and final state total energies, and utilize standard nucleon vector and axial-vector on-shell form factors. Many of these model parameters may be inferred from existing data; for example, p_F , E_B , and the vector form factors can be determined from elastic electron scattering data [4,5]. Despite providing these constraints, electron data yield limited information on the axial-vector form factor of the nucleon and the CCQE cross section at very low four-momentum transfer (Q^2). Present knowledge of the axial-vector form factor has been informed largely by past neutrino experiments, but these suffer from low statistics and were performed using predominantly deuterium targets [6]. Since these early measurements, neutrino experiments have encountered difficulties describing their data at low Q^2 , where nuclear effects are largest, and have often measured axial-vector form factor parameters above some minimum Q^2 value.

The MiniBooNE experiment has collected the largest sample of low energy muon neutrino CCQE events to date. We describe here the use of such events in tuning the RFG model to better describe quasielastic scattering on nuclear targets. The analysis fits the reconstructed Q^2 distribution of the MiniBooNE CCQE data in the region $0 < Q^2 < 1 \text{ GeV}^2$ to a simple RFG model [3] with two adjustable parameters: the axial mass M_A appearing in the axial-vector form factor and κ , a parameter that adjusts the level of Pauli blocking at low values of Q^2 . The best-fit model results in a good description of the data across the full kinematic phase space including the low- Q^2 region. This technique is crucial to the MiniBooNE oscillation search [1] as it is used to predict the ν_e CCQE oscillation events based on the constraints provided by the high-statistics MiniBooNE ν_μ CCQE sample.

The Fermilab Booster neutrino beam, optimized for the MiniBooNE oscillation search, is particularly suited for investigation of low energy neutrino interactions. The Fermilab Booster provides 8.89 GeV/ c protons which collide with a 71 cm long beryllium target inside a magnetic horn. The horn focuses positively charged pions and kaons produced in these collisions, which can subsequently decay in a 50 m long decay region, yielding an intense flux of muon neutrinos. A GEANT4-based [7] beam simulation uses a parametrization [8] of pion production cross sections based on recent measurements from the HARP [9] and E910 [10] experiments, along with a detailed model of the beam line geometry to predict the neutrino flux as a function of neutrino energy and flavor. The resulting flux of neutrinos at the MiniBooNE detector is predicted to be 93.8% (5.7%) ν_μ ($\bar{\nu}_\mu$) with a mean energy of ~ 700 MeV. Because 99% of the flux lies below 2.5 GeV, the background from high multiplicity neutrino interactions is small. Approximately 40% of the total events at MiniBooNE are predicted to be ν_μ CCQE, of which 96% result from pion decays in the beam.

The MiniBooNE detector is a spherical tank of inner radius 610 cm filled with 800 tons of mineral oil (CH_2), situated 541 m downstream of the proton target. An optical barrier divides the detector into two regions, an inner volume with a radius of 575 cm and an outer volume 35 cm thick. The inner region of the tank houses 1280 inward-facing 8 in. photomultiplier tubes (PMTs), providing 10% photocathode coverage. The outer region is lined with 240 pair-mounted PMTs which provide a veto for charged particles entering or leaving the tank. Muons produced in CCQE interactions emit primarily Cherenkov light with a small amount of scintillation light. A large number of muons stop and decay in the main detector volume. The muon kinetic energy resolution is 7% at 300 MeV and the angular resolution is 5° . The response of the detector to muons is calibrated using a dedicated muon tagging system that independently measures the muon energy for cosmic ray muons ranging up to 800 MeV.

Neutrino interactions within the detector are simulated with the V3 NUANCE event generator [11]. This program provides the framework for tuning the CCQE cross section parameters (described below) and predicts backgrounds to the sample, including neutrino induced single pion production events [charged current (CC) 1π]. Pion interactions in the nucleus and photon emission from nuclear deexcitation in NUANCE are tuned to reproduce MiniBooNE and other [12] data. A GEANT3-based [13] detector model (with G4CALOR [14] hadronic interactions) simulates the detector response to particles produced in neutrino interactions. The simulation of light production and propagation in mineral oil has been tuned using external small-sample measurements [15], muon decay electrons (also used to calibrate the energy scale), and recoil nucleons from neutrino neutral current (NC) elastic scattering events. The predicted events are additionally overlaid with events measured in a beam-off gate, in order to incorporate backgrounds from natural radioactivity and cosmic rays into the simulated data.

Because of the low energy neutrino beam and MiniBooNE detector capabilities, the identification of ν_μ CCQE interactions relies solely on the detection of the primary muon and associated decay electron in these events:

$$\nu_\mu + n \rightarrow \mu^- + p, \quad \mu^- \rightarrow e^- + \nu_\mu + \bar{\nu}_e.$$

This simple selection is highly effective for several reasons. First, the efficiency for detecting the decay of the μ^- produced in such events is high, 83%. The losses are due to muon capture on carbon (8% [16]) and insufficient decay time or energy of the decay electron (10%). Second, the CC $1\pi^+$ contamination is significantly reduced by requiring a single decay electron, since CC $1\pi^+$ events typically yield two decay electrons, one each from the primary muon and the π^+ decay chains. The exceptions are cases in

which the primary μ^- is captured or, more likely, the π^+ is either absorbed or undergoes a charge-changing interaction in the target nucleus or detector medium. Each of these processes is included in the detector simulation. Finally, by avoiding requirements on the outgoing proton kinematics, the selection is inherently less dependent on nuclear models.

Timing information from the PMTs allows the light produced by the initial neutrino interaction (first “subevent”) to be separated from light produced by the decay electron (second subevent). The time and charge response of the PMTs is used to reconstruct the position, kinetic energy, and direction vector of the primary particle within each subevent. Once separated into subevents, we require that the first subevent (the neutrino interaction) must occur in coincidence with a beam pulse, have a reconstructed position <500 cm from the center of the detector, possess <6 veto-PMT hits to ensure containment, and have >200 main-PMT hits to avoid electrons from cosmic ray muon decays. The second subevent (the μ^- decay electron) must have <6 veto-PMT hits and <200 main-PMT hits. Subsequent cuts specifically select ν_μ CCQE events and discriminate against CC $1\pi^+$ backgrounds. First, events must contain exactly two subevents. Second, the distance between the electron vertex and muon track end point must be less than 100 cm, ensuring that the decay electron is associated with the muon track.

A total of 193 709 events pass the MiniBooNE ν_μ CCQE selection criteria from 5.58×10^{20} protons on target collected between August 2002 and December 2005. The cuts are estimated to be 35% efficient at selecting ν_μ CCQE events in a 500 cm radius, with a CCQE purity of 74%. The 35% efficiency is the product of a 50% probability for containing events within the tank, the aforementioned 83% muon decay detection efficiency, and an 85% efficiency for the electron vertex to muon end point requirement.

The predicted backgrounds are 75% CC $1\pi^+$, 15% CC $1\pi^0$, 4% NC $1\pi^\pm$, 3% CC multi- π , 1% NC elastic, 1% $\bar{\nu}_\mu$ CC $1\pi^-$, 1% NC $1\pi^0$, $<1\%$ $\eta/\rho/K$ production, and $<1\%$ deep inelastic scattering and other events [11]. In the analysis, cross section uncertainties of 25%, 40%, and 25% are assumed on the 1π , multi- π plus $\eta/\rho/K$ production, and deep inelastic scattering backgrounds, respectively. Because pions can be absorbed via final state interactions in the target nucleus, a large fraction of the background events look like CCQE events in the MiniBooNE detector. “CCQE-like” events, all events with a muon and no pions in the final state, are predicted to be 84% of the sample after cuts.

The observables in the MiniBooNE ν_μ CCQE sample are the muon kinetic energy T_μ and the muon angle with respect to the neutrino beam direction θ_μ . The high-statistics MiniBooNE data sample allows us to verify the simulation in two dimensions. Figure 1 shows the level of

agreement between the shape of the data and simulation in the CCQE kinematic quantities before any CCQE cross section model adjustments. For this comparison, the simulation assumes the RFG model as implemented in NUANCE [3,11], with $E_B = 34$ MeV [4], $p_F = 220$ MeV/c [4], updated nondipole vector form factors [5], and a nonzero pseudoscalar form factor [17]. The axial-vector form factor is assumed to have a dipole form as a function of Q^2 with one adjustable parameter, M_A , the so-called “axial mass,” $F_A(Q^2) = g_A/(1 + Q^2/M_A^2)^2$.

The simulation shown in Fig. 1 specifically assumes $g_A = 1.2671$ [18] and $M_A = 1.03$ GeV [19]. These model parameters are common defaults in most neutrino simulations. The figure shows that the disagreement between data and simulation follows lines of constant Q^2 and not E_ν . This supports the assumption that the data-model disagreement is not due to a mismodeling of the incoming neutrino energy spectrum but an inaccuracy in the simulation of the CCQE process itself. We also explicitly assume no ν_μ disappearance due to oscillations.

Guided by indications that the data-model discrepancy is only a function of Q^2 , we have modified the existing ν_μ CCQE model rather than introduce more drastic changes to the cross section calculation. This approach works well and requires adjustment of only two parameters: M_A and E_{10} . The parameter E_{10} effectively controls the effect of Pauli blocking. It is the lower bound of integration over initial state nucleon energy and appears within the RFG model together with an upper bound E_{hi} :

$$E_{hi} = \sqrt{p_F^2 + M_n^2}, \quad E_{10} = \sqrt{p_F^2 + M_p^2} - \omega + E_B, \quad (1)$$

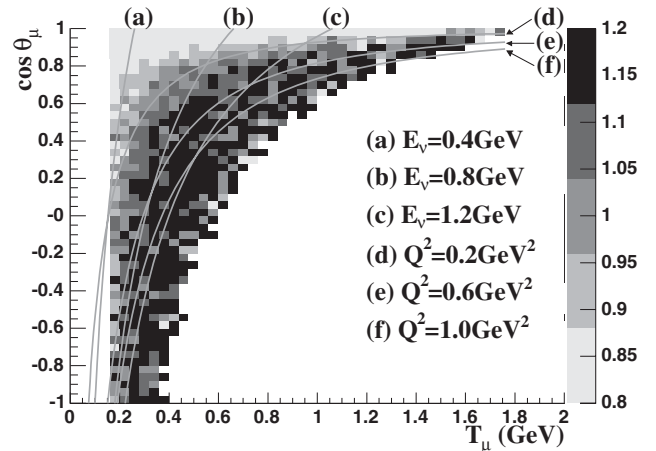


FIG. 1. Ratio of MiniBooNE ν_μ CCQE data or simulation as a function of reconstructed muon angle and kinetic energy. The prediction is prior to any CCQE model adjustments and has been normalized to the data. The $\chi^2/\text{dof} = 79.5/53$. The ratio forms a 2D surface whose values are represented by the gray scale, shown on the right. If the simulation modeled the data perfectly, the ratio would be unity everywhere. Contours of constant E_ν and Q^2 are overlaid, and only bins with >20 events in the data are plotted.

where M_n is the target neutron mass, M_p is the outgoing proton mass, and ω is the energy transfer. In the RFG model, E_{hi} is the energy of an initial nucleon on the Fermi surface and E_{lo} is the lowest energy of an initial nucleon that leads to a final nucleon just above the Fermi momentum (and thus obeying the exclusion principle in the final state). In practice, a simple scaling of E_{lo} was implemented in the MiniBooNE CCQE data fit via $E_{lo} = \kappa(\sqrt{p_F^2 + M_p^2} - \omega + E_B)$. The parameter κ adds a degree of freedom to the RFG model which can describe the smaller cross section observed in the data at low momentum transfer and is likely compensating for the naive treatment of Pauli blocking in the RFG model.

The adjusted RFG model is then fit to the shape of the reconstructed Q^2 distribution in the MiniBooNE ν_μ CCQE data:

$$Q^2 = -q^2 = -m_\mu^2 + 2E_\nu(E_\mu - p_\mu \cos\theta_\mu) > 0, \quad (2)$$

where m_μ is the muon mass, E_μ (p_μ) is the reconstructed muon energy (momentum), and θ_μ is the reconstructed muon scattering angle. The reconstructed neutrino energy E_ν is formed assuming the target nucleon is at rest inside the nucleus:

$$E_\nu = \frac{2(M_n - E_B)E_\mu - (E_B^2 - 2M_nE_B + m_\mu^2 + \Delta M^2)}{2[(M_n - E_B) - E_\mu + p_\mu \cos\theta_\mu]}, \quad (3)$$

where $\Delta M^2 = M_n^2 - M_p^2$ and $E_B > 0$. A small correction is applied to E_ν in both data and simulation to account for the biasing effects of Fermi smearing. This procedure, while yielding a more accurate E_ν estimate, has a negligible impact on the Q^2 fit to MiniBooNE CCQE data. These expressions, with reconstructed muon kinematics, yield an E_ν resolution of 11% and a Q^2 resolution of 21% for CCQE events.

The model parameters M_A and κ are obtained from a least-squares fit to the measured data in 32 bins of reconstructed Q^2 from 0 to 1 GeV^2 . All other parameters of the model are held fixed to the values listed previously, and a complete set of correlations between systematic uncertainties is considered. The total prediction is normalized to the data for each set of parameter values. Thus, the procedure is sensitive only to the shape of the Q^2 distribution, and any changes in the total cross section due to parameter variation do not impact the quality of fit. The Q^2 distributions of data and simulation before and after the fitting procedure are shown in Fig. 2. The χ^2/dof of the fit is 32.8/30 and the parameters extracted from the MiniBooNE ν_μ CCQE data are

$$M_A^{\text{eff}} = 1.23 \pm 0.20 \text{ GeV}, \quad (4)$$

$$\kappa = 1.019 \pm 0.011. \quad (5)$$

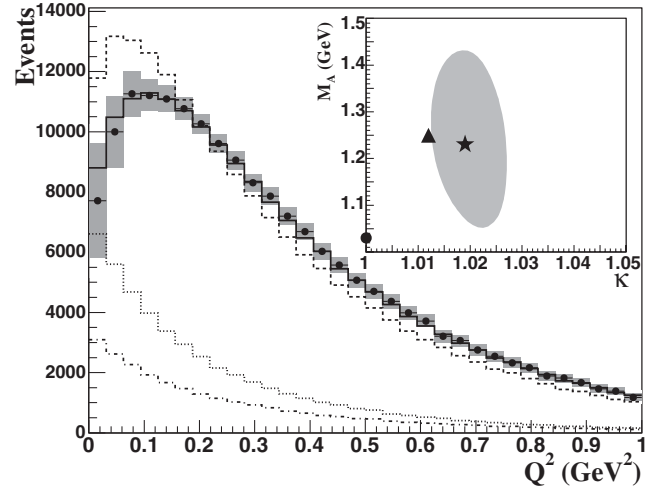


FIG. 2. Reconstructed Q^2 for ν_μ CCQE events including systematic errors. The simulation, before (dashed curve) and after (solid curve) the fit, is normalized to data. The dotted curve (dot-dashed curve) shows backgrounds that are not CCQE (not “CCQE-like”). The inset shows the 1σ C.L. contour for the best-fit parameters (star), along with the starting values (circle), and fit results after varying the background shape (triangle).

While normalization is not explicitly used in the fit, the new model parameters increase the predicted rate of ν_μ CCQE events at MiniBooNE by 5.6%. The ratio of detected events to predicted, with the best-fit CCQE model parameters, is 1.21 ± 0.24 .

In general, varying M_A allows us to reproduce the high Q^2 behavior of the observed data events. A fit for M_A above $Q^2 > 0.25 \text{ GeV}^2$ yields consistent results, $M_A^{\text{eff}} = 1.25 \pm 0.12 \text{ GeV}$. However, fits varying only M_A across the entire Q^2 range leave considerable disagreement at low Q^2 ($\chi^2/\text{dof} = 48.8/31$). The Pauli-blocking parameter κ is

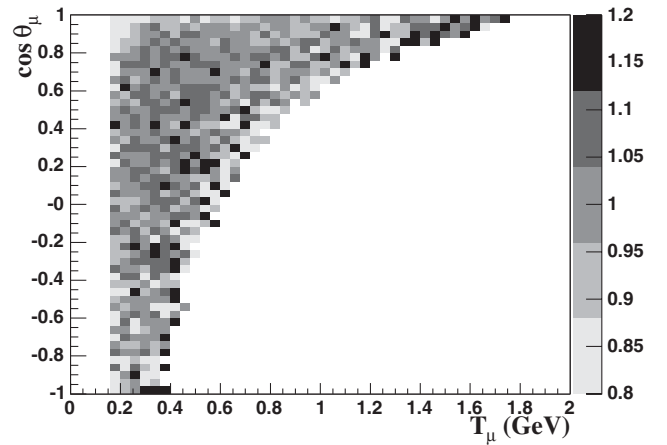


FIG. 3. Ratio of data or simulation as a function of muon kinetic energy and angle after CCQE model adjustments. The simulation has been normalized to the data. The $\chi^2/\text{dof} = 45.1/53$. Compare to Fig. 1.

TABLE I. Uncertainties in M_A^{eff} and κ from the fit to MiniBooNE ν_μ CCQE data. The total error is not a simple quadrature sum due to correlations between the Q^2 bins created by the systematic uncertainties.

Error source	δM_A^{eff}	$\delta \kappa$
Data statistics	0.03	0.003
Neutrino flux	0.04	0.003
Neutrino cross sections	0.06	0.004
Detector model	0.10	0.003
CC π^+ background shape	0.02	0.007
Total error	0.20	0.011

instrumental here, enabling this model to match the behavior of the data down to $Q^2 = 0$ (Fig. 2).

Figure 3 shows the agreement between data and simulation after incorporation of the M_A and κ values from the Q^2 fit to MiniBooNE data. Comparing to Fig. 1, the improvement is substantial and the data are well described throughout the kinematic phase space.

Table I shows the contributions to the systematic uncertainties on M_A and κ . The detector model uncertainties dominate the error in M_A due to their impact on the energy and angular reconstruction of CCQE events in the MiniBooNE detector. The dominant error on κ is the uncertainty in the Q^2 shape of background events. This error (not included in the contour of Fig. 2) is evaluated in a separate fit, where MiniBooNE CC $1\pi^+$ data are used to set the background instead of the event generator prediction, and then added in quadrature.

The result reported here, $M_A^{\text{eff}} = 1.23 \pm 0.20$ GeV, is consistent with a recent K2K measurement on a water target, $M_A = 1.20 \pm 0.12$ GeV [20]. Both values are consistent with but higher than the historical value, $M_A = 1.026 \pm 0.021$ GeV, set largely by deuterium-based bubble chamber experiments [19]. The M_A value reported here should be considered an “effective parameter” in the sense that it may be incorporating nuclear effects not otherwise included in the RFG model. In particular, it may be that a more proper treatment of the nucleon momentum distribution in the RFG would yield an M_A value in closer agreement to that measured on deuterium. Future efforts will therefore explore how the value of M_A extracted from the MiniBooNE data is altered upon replacement of the RFG model with more advanced nuclear models [21].

In summary, modern quasielastic scattering data on nuclear targets are revealing the inadequacies of present neutrino cross section simulations. Taking advantage of the high-statistics MiniBooNE ν_μ CCQE data, we have ex-

tracted values of an effective axial mass parameter, $M_A^{\text{eff}} = 1.23 \pm 0.20$ GeV, and a Pauli-blocking parameter, $\kappa = 1.019 \pm 0.011$, achieving substantially improved agreement with the observed kinematic distributions in this data set. Incorporation of both fit parameters allows, for the first time, a description of neutrino CCQE scattering on a nuclear target down to $Q^2 = 0$ GeV².

We wish to acknowledge the support of Fermilab, the Department of Energy, and the National Science Foundation in the construction, operation, and data analysis of the MiniBooNE experiment.

- [1] A. A. Aguilar-Arevalo *et al.* (MiniBooNE Collaboration), Phys. Rev. Lett. **98**, 231801 (2007).
- [2] S. Yamamoto *et al.* (K2K Collaboration), Phys. Rev. Lett. **96**, 181801 (2006).
- [3] R. A. Smith and E. J. Moniz, Nucl. Phys. **B43**, 605 (1972); **B101**, 547 (1975).
- [4] E. J. Moniz *et al.*, Phys. Rev. Lett. **26**, 445 (1971); the binding energy is 25 MeV from electron scattering data plus 9 MeV from the $T = 0, 1$ splitting plus Coulomb corrections.
- [5] R. Bradford *et al.*, Nucl. Phys. B, Proc. Suppl. **159**, 127 (2006).
- [6] S. K. Singh and E. Oset, Nucl. Phys. **A542**, 587 (1992).
- [7] S. Agostinelli *et al.*, Nucl. Instrum. Methods Phys. Res., Sect. A **506**, 250 (2003).
- [8] J. R. Sanford and C. L. Wang, BNL AGS Internal Reports No. 11299 and 11479 (unpublished).
- [9] M. G. Catanesi *et al.*, Eur. Phys. J. C **52**, 29 (2007).
- [10] I. Chemakin *et al.*, arXiv:0707.2375v1 [Phys. Rev. C (to be published)].
- [11] D. Casper, Nucl. Phys. B, Proc. Suppl. **112**, 161 (2002).
- [12] D. Ashery *et al.*, Phys. Rev. C **23**, 2173 (1981); H. Ejiri, Phys. Rev. C **48**, 1442 (1993); F. Ajzenberg-Selove, Nucl. Phys. **A506**, 1 (1990).
- [13] CERN Program Library Long Writeup Report No. W5013, 1993.
- [14] C. Zeitnitz and T. A. Gabriel, Nucl. Instrum. Methods Phys. Res., Sect. A **349**, 106 (1994).
- [15] B. C. Brown *et al.*, IEEE Nucl. Sci. Symp. Conf. Rec. **1**, 652 (2004).
- [16] T. Suzuki *et al.*, Phys. Rev. C **35**, 2212 (1987).
- [17] K. F. Liu *et al.*, Phys. Rev. Lett. **74**, 2172 (1995).
- [18] W. M. Yao *et al.*, J. Phys. G **33**, 1 (2006).
- [19] V. Bernard *et al.*, J. Phys. G **28**, R1 (2002).
- [20] R. Gran *et al.* (K2K Collaboration), Phys. Rev. D **74**, 052002 (2006).
- [21] J. E. Amaro *et al.*, Phys. Rev. C **71**, 015501 (2005); T. Leitner *et al.*, Phys. Rev. C **73**, 065502 (2006); O. Benhar *et al.*, Phys. Rev. D **72**, 053005 (2005); S. Ahmad *et al.*, Phys. Rev. D **74**, 073008 (2006).